

Large ordered arrays of single photon sources based on II-VI semiconductor colloidal quantum dot

Qiang Zhang¹, Cuong Dang^{2†}, Hayato Urabe^{1†}, Jing Wang², Shouheng Sun³, and Arto Nurmikko^{1,2*}

¹Division of Engineering, Brown University, Providence, Rhode Island 02912, USA

²Department of Physics, Brown University, Providence, Rhode Island 02912, USA

³Department of Chemistry, Brown University, Providence, Rhode Island 02912, USA

[†]These authors made equal contributions to this work.

*Corresponding author: arto_nurmikko@brown.edu

Abstract: In this paper, we developed a novel and efficient method of deterministically organizing colloidal particles on structured surfaces over macroscopic areas. Our approach utilizes integrated solution-based processes of dielectric encapsulation and electrostatic-force-mediated self-assembly, which allow precisely controlled placement of sub-10nm sized particles at single particle resolution. As a specific demonstration, motivated by application to single photon sources, highly ordered 2D arrays of single II-VI semiconductor colloidal quantum dots (QDs) were created by this method. Individually, the QDs display triggered single photon emission at room temperature with characteristic photon antibunching statistics, suggesting a pathway to scalable quantum optical radiative systems.

©2008 Optical Society of America

OCIS codes: (230.5590) Quantum-well, -wire and -dot devices; (270.5290) Photon Statistics; (160.4236) Nano materials

References and links

1. Y. N. Xia, B. Gates, and S. H. Park, "Fabrication of three-dimensional photonic crystals for use in the spectral region from ultraviolet to near-infrared," *J. Lightwave Technol.* **17**, 1956–1962 (1999).
2. S. Coe, W.-K. Woo, M. Bawendi, and V. Bulovi, "Electroluminescence from single monolayers of nanocrystals in molecular organic devices," *Nature* **420**, 800–803 (2002).
3. S.-W. Chung, D. S. Ginger, M. W. Morales, Z. Zhang, V. Chandrasekhar, M. A. Ratner, and C. A. Mirkin, "Top-down meets bottom-up: dip-pen nanolithography and DNA-directed assembly of nanoscale electrical circuits," *Small* **1**, 64–69 (2005).
4. R. J. Tseng, C. Tsai, L. Ma, J. Ouyang, C. S. Ozkan, and Y. Yang, "Digital memory device based on tobacco mosaic virus conjugated with nanoparticles," *Nature Nanotech.* **1**, 72–77 (2006).
5. S. Sun, C. B. Murray, D. Weller, L. Folks, and A. Moser, "Monodisperse FePt nanoparticles and ferromagnetic FePt nanocrystal superlattices," *Science* **287**, 1989–1992 (2000).
6. M. F. Ali, et al. "DNA hybridization and discrimination of single-nucleotide mismatches using chip-based microbead arrays," *Anal. Chem.* **75**, 4732–4739 (2003).
7. B. Lounis, and M. Orrit, "Single-photon sources," *Rep. Prog. Phys.* **68**, 1129–1179 (2005).
8. A. J. Shields, "Semiconductor quantum light sources," *Nature Photon.* **1**, 215–223 (2007).
9. P. Michler, "A quantum dot single-photon turnstile device," *Science* **290**, 2282–2285 (2000).
10. S. Strauf, P. Michler, M. Klude, D. Hommel, G. Bacher, and A. Forchel, "Quantum optical studies on individual acceptor bound excitons in a semiconductor," *Phys. Rev. Lett.* **89**, 177403 (2002).
11. C. Kurtsiefer, S. Mayer, P. Zarda, and H. Weinfurter, "Stable solid-state source of single photons," *Phys. Rev. Lett.* **85**, 290–293 (2000).
12. P. Michler, A. Imamoglu, M. D. Mason, P. J. Carson, G. F. Strouse, and F. K. Buratto, "Quantum correlation among photons from a single quantum dot at room temperature," *Nature* **406**, 968–970 (2000).
13. C. B. Murray, D. J. Norris, and M. G. Bawendi, "Synthesis and characterization of nearly monodisperse CdE (E = S, Se, Te) semiconductor nanocrystallites," *J. Am. Chem. Soc.* **115**, 8706–8715 (1993).
14. V. I. Klimov, A. A. Mikhailovsky, D. W. McBranch, C. A. Leatherdale, and M. G. Bawendi, "Quantization of multiparticle Auger rates in semiconductor quantum dots," *Science* **287**, 1011–1013 (2000).

15. L.-W. Wang, M. Califano, A. Zunger, and A. Franceschetti, "Pseudopotential theory of Auger processes in CdSe quantum dots," *Phys. Rev. Lett.* **91**, 056404 (2003).
16. B. Lounis, H. A. Bechtel, D. Gerion, P. Alivisatos, and W. W. Moerner, "Photon antibunching in single CdSe/ZnS quantum dot fluorescence," *Chem. Phys. Lett.* **329**, 399-404 (2000).
17. X. Brokmann, E. Giacobino, M. Dahan, and J. P. Hermier, "Highly efficient triggered emission of single photons by colloidal CdSe/ZnS nanocrystals," *Appl. Phys. Lett.* **85**, 712-714 (2004).
18. Y. Min, M. Akbulut, K. Kristiansen, Y. Golan, and J. Israelachvili, "The role of interparticle and external forces in nanoparticle assembly," *Nature Mater.* **7**, 527-538 (2008).
19. Y. Yin, Y. Lu, B. Gates, and Y. Xia, "Template-assisted self-assembly: a practical route to complex aggregates of monodispersed colloids with well-defined sizes, shapes, and structures," *J. Am. Chem. Soc.* **123**, 8718-8729 (2001).
20. Y. Cui, M. T. Björk, J. A. Liddle, C. Sönnichsen, B. Boussert, and A. P. Alivisatos, "Integration of colloidal nanocrystals into lithographically patterned devices," *Nano. Lett.*, **4**, 1093-1098 (2004).
21. T. Kraus, L. Malaquin, H. Schmid, W. Riess, N. D. Spencer, and H. Wolf, "Nanoparticle printing with single-particle resolution," *Nature Nanotech.* **2**, 570-576 (2007).
22. R. Xie, U. Kolb, J. Li, T. Basche, and A. Mews, "Synthesis and Characterization of Highly Luminescent CdSe-Core CdS/Zn_{0.5}Cd_{0.5}S/ZnS Multishell Nanocrystals," *J. Am. Chem. Soc.* **127**, 7480-7488 (2005).
23. J. J. Li, Y. A. Wang, W. Z. Guo, J. C. Keay, T. D. Mishima, M. B. Johnson, and X. P. Peng, "Large-scale synthesis of nearly monodisperse CdSe/CdS core/shell nanocrystals using air-stable reagents via successive ion layer adsorption and reaction," *J. Am. Chem. Soc.* **125**, 12567-12575 (2003).
24. B. Mahler, P. Spinicelli, S. Buil, X. Quelin, J.-P. Hermier, and B. Dubertret, "Towards non-blinking colloidal quantum dots," *Nature Mater.* **7**, 659-664 (2008).
25. F. J. Arriagada, and K. Osseo-Asare, "Synthesis of nanosize silica in a nonionic water-in-oil microemulsion: effects of the water/surfactant molar ratio and ammonia concentration," *J. Colloid Interface Sci.* **211**, 210-220 (1999).
26. P. L. Luisi, and B. E. Straub, *Reverse Micelles* (Plenum, New York, 1984).
27. S. T. Selvan, T. T. Tan, and J. Y. Ying, "Robust, non-cytotoxic, silica-coated CdSe quantum dots with efficient photoluminescence," *Adv. Mater.* **17**, 1620-1625 (2005).
28. M. Darbandi, R. Thomann, and T. Nann, "Single quantum dots in silica spheres by microemulsion synthesis," *Chem. Mater.* **17**, 5720-5725 (2005).
29. D. K. Yi, S. S. Lee, G. C. Papaefthymiou, and J. Y. Ying, "Nanoparticle architectures templated by SiO₂/Fe₂O₃ nanocomposites," *Chem. Mater.* **18**, 614-619 (2006).
30. J. Aizenberg, P. V. Braun, and P. Wiltzius, "Patterned colloidal deposition controlled by electrostatic and capillary forces," *Phys. Rev. Lett.* **84**, 2997-3000 (2000).
31. R. J. Mashl, N. Grönbech-Jensen, M. R. Fitzsimmons, M. Lütt, and D. Li, "Theoretical and experimental adsorption studies of polyelectrolytes on an oppositely charged surface," *J. Chem. Phys.* **110**, 2219-2225 (1999).
32. S. A. Empedocles, R. Neuhauser, K. Shimizu, and M. G. Bawendi, "Photoluminescence from single semiconductor nanostructures," *Adv. Mater.* **11**, 1243-1256 (1999).

1. Introduction

Ordered assemblies of mesoscopic scale colloid particles are an important class of nanomaterials that provide means to achieve one, two and three dimensional structures for a wide variety of applications, ranging from photonics devices [1,2] to microelectronics [3], memory [4], storage [5] and sensor [6] type of devices, etc. In order to fulfill their potential, it is a prerequisite to understand and gain control over the relevant growth and ordering parameters of the underlying nanometric building units. This becomes increasingly challenging when the particle size migrates into the quantum regime and the desired functional properties are yet only apparent at the individual particle level, requiring the need for precise placement of nanoparticles at single particle resolution.

In specific application areas of quantum key distribution and quantum computing, the development of practical non-classical light sources [7,8] is a vigorous subject of ongoing research. A number of reports have appeared recently, demonstrating how single photon emission can be possible in solid state systems [9-12]. Among them, II-VI semiconductor colloidal QDs are highly fluorescent nanocrystals which are prepared through organometallic synthesis [13] in solution phase. Recent discoveries show that the suppression of biexciton and multiexciton emissions in CdSe-based QDs can be quite effective, as a result of the enhanced non-radiative Auger recombination processes [14,15] with respect to their bulk counterpart. It follows that the lowest quasi-zero dimensional Wannier exciton state radiates

much like a two-level atomic system, making the colloidal QDs one appealing material

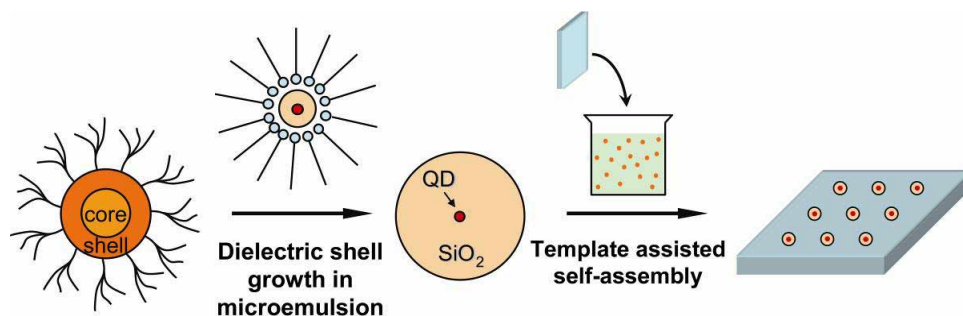


Fig. 1. (Media 1) Indirect self-assembly of surface-engineered nanoparticles. First, uniformly thick shells of optically transparent dielectric material (silica) are grown onto the nanoparticle “seeds” in microemulsion, which is illustrated here as CdSe-based core-shell colloidal QDs; then, the resulted composite particles, each containing a single QD, are individually anchored onto lithographically defined templates by electrostatic force self-assembly in solution.

candidate as *room-temperature-operating* single photon source [16,17], owing to its large exciton binding energy commonly seen in II-VI compounds. To exploit such property in practice, integration of the QDs at well-defined position within functional photonic device structures is a prerequisite. However, their translation to device implementation is currently hampered by the lack of precise spatial control of individual emitters on solid surfaces at macroscopic scale.

Thermodynamically driven self-assembly is an efficient method capable of arranging large number of colloidal particles in parallel to create complex nanostructures. It has been explored extensively on the basis of a variety of interparticle and external forces [18]. However, precise and reproducible organization of small nanoparticles into versatile geometries with long range order poses severe challenges in controlling the particle-particle and particle-substrate interactions. Perhaps the most promising approach so far is based on capillary forces [19], which has demonstrated large-area high resolution patterning of metallic particles down to 50nm in size [20,21]. But its susceptibility to the influence of thermal (Brownian motion) effect in solution has rendered this method ineffective for particles of even smaller size and lighter mass, such as QDs. The sensitivity on detailed solvent hydrodynamic properties also makes it hard to apply to particles suspended in nonaqueous solutions.

Here, we report on a way to overcome these limitations by resorting to indirect self-assembly approach in conjunction with efficacious surface engineering of the nanoparticles in process. Our approach starts with the well-established solution-based synthesis of II-VI colloidal QDs, but now follows the key idea of adapting their surface chemistry so as to substantially enlarge these optically active “seed” nanoparticles by the subsequent growth of a thick (about 100 nm) optically transparent (passive) dielectric shell. The enlarged particles, each containing a single QD, are then individually self-assembled onto pre-defined templates by employing an electrostatic “adhesion” approach. In the end, the process results in geometrically precise planar 2D arrays of silica-clad QDs with controlled spatial specificity of location. In broad terms, we symbiotically combine the so-called “bottom-up” and “top-down” fabrication approaches, as illustrated in Fig. 1.

2. QD array fabrication and characterization

2.1 QD encapsulation

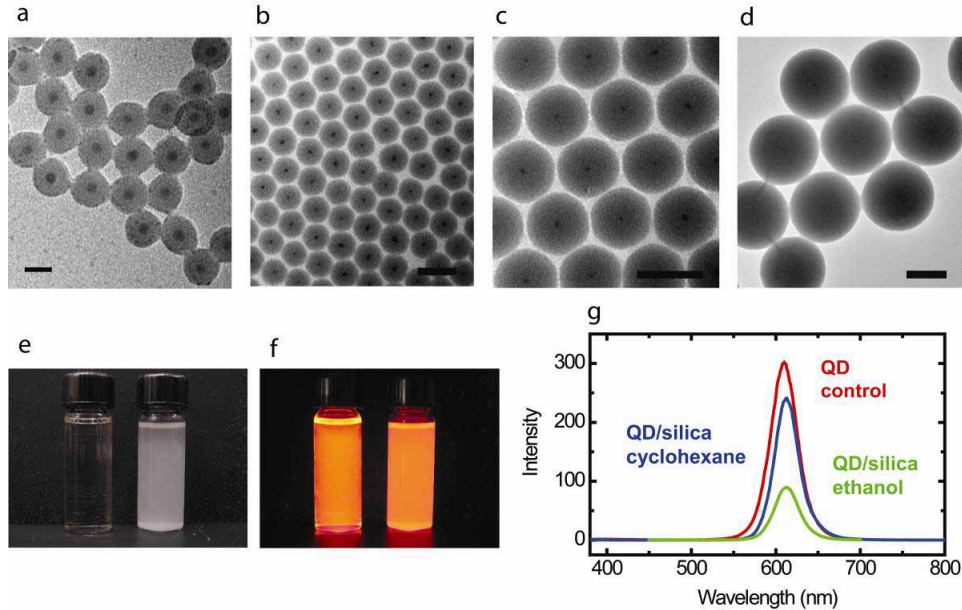


Fig. 2. (Media 2) Silica-encapsulated II-VI semiconductor colloidal QDs. a-d, Transmission electron microscope images of the synthesized silica-clad QDs with various total particle diameters of 28nm (a), 75nm (b), 95nm (c), and 180nm (d), obtained via microemulsion synthesis with NP-5 (a) and NP-12 (b-d) as the surfactants, respectively. Single QDs of about 8nm in diameter are visible at the core of the composite particles, appearing as small dark dots. The scale bars in the images correspond to 20nm (a) and 100nm (b-d). e,f, the synthesized silica-clad QDs (right, 180nm diameter) in cyclohexane under ambient (e) and UV (f) exposures. Bare QD controls (left) with similar concentration was used as a reference. g, photoluminescence spectra of the silica-clad QDs in cyclohexane (blue) and in ethanol (green), in comparison to the bare QD control (red), under the excitation at 380nm.

The CdSe-core CdS/Zn_{0.5}Cd_{0.5}S/ZnS-multishell QDs used in this study were synthesized following a procedure described in Ref. 22, in which the core was formed by precipitation reaction first and then the desired multishell growth was achieved by successive ion layer adhesion and reaction (SILAR) technique [23]. The as-synthesized QDs were capped with octadecylamine (ODA). They had an averaged diameter of 8nm and measured fluorescent quantum yield of about 50%. Individual QDs exhibited the typical blinking widely reported; however in terms of main goal of this paper we did not attempt to control or reduce this behavior. We do note that recent results report significant reduction or elimination of blinking [24]. A thick shell of silica was subsequently grown onto the QD utilizing water-in-oil (W/O) microemulsion growth technique, which has been widely adopted to synthesize silica colloidal particles, but so far mainly in the sub-100nm size range [25]. The microemulsion process began in a non-polar solvent (cyclohexane) in which the ODA-capped QDs and an excessive amount of non-ionic surfactant polyoxyethylene(12) nonylphenyl ether (NP-12) were dissolved, which typically contains 1.5-24nM QDs, 167mM NP-12, and 797mM hexanol. Adding a slight amount (105mM) of NH₄OH aqueous solution (30 wt.%) triggered the spontaneous formation of reverse micelles [26]. Through interaction with the reverse micelles, the loosely bonded ODA molecules tended to leave the QD's surface, driving the QDs into the reverse micelles in a one-to-one correspondence. The micelles then behaved as a micro-reactor where polycondensation of the hydrolyzed silica precursor tetraethyl orthosilicate

(TEOS) took place and nucleated onto the QDs. The reaction started when 41mM of TEOS was applied dropwise and it was allowed to proceed for 8 hours before the particles were isolated by centrifugal precipitation. The thickness of the silica shell can be effectively tuned by controlling the concentrations of the QDs and/or of the TEOS. Similar silica-cladding approaches have recently been initiated on QDs [27,28] as well as on magnetic nanoparticles [29], but issues related to particle size control and encapsulation uniformity are reported to be considerable challenges. However, by our technique, we have achieved significant improvement in the final particle size distribution, as seen from the transmission electron microscope (TEM) images in Fig. 2(a)-2(d) where up to 95% of the particles have single QD core precisely positioned at the center. One key to this advance is the choice of the surfactant NP-12 with relatively large unit length polyoxyethylene hydrophilic group. As NP-12 helps to reinforce the stability of the micelle against ethanol, a by-product of the reaction, we could tune the final particle size up to 220nm in a *one-pot synthesis* without generating secondary silica nuclei. Nevertheless, shorter polyoxyethylene surfactant, such as polyoxyethylene(5) nonylphenyl ether (NP-5), is still useful to obtain thin silica shells with thickness below 15nm (Fig. 2(a)).

Important for applications, the optical quality of the QDs is largely preserved after thick silica encapsulation, attributed to the improved QD crystallinity and photochemical stabilities [22] offered by the graded multishell synthesis approach in comparison to the traditional single ZnS shell structure. As seen in Fig. 2(g), the photoluminescence (PL) spectrum of the QDs after silica encapsulation shows clean QD ground state exciton emission signature centered around 613nm (slightly red-shifted by about 3nm compared to the “bare” QD control), without introducing any noticeable impurity emission background. The PL efficiency of the silica-clad QDs is nearly unchanged if they are dispersed in non-polar solvent; however, it drops by about 60% upon transferring into ethanol in which the final 2D assembly process is carried out (described next). This effect is primarily because of the incomplete passivation of the QD surface as a result of the porosity of the silica material grown by the current method, an issue that we anticipate to address in future work.

2.2 Self-assembly of the encapsulated QDs

In order to achieve the goal of controlled spatial organization of individual silica-clad QDs, we developed an electrostatic force self-assembly method (abbreviated as EFSA in this paper) whose process flow is sketched in Fig. 3(a)-3(e). The EFSA approach relies on utilizing the electrostatic interactions between the silica-clad QDs and an oppositely charged polyelectrolyte template whose principle has been demonstrated previously with micrometer-sized particles [30]. It is implemented here as follows. First, a template consisting of an array of SiO₂ circular pads, defining the capture sites for the particles, was created on a silicon substrate, using electron-beam lithography followed by SiO₂ deposition and lift-off. Prior to lift-off, a monolayer of cationic polyelectrolyte poly(diallyldimethylammonium chloride) (PDDA) was self-assembled [31] onto the top surface of the pads by dipping into a PDDA aqueous solution for 20mins, which contains a mixture of PDDA (molecular weight 400K-500K) 0.58mM and NaCl 0.5M with pH value of 7.0. Then, immersion of the templates into the ethanol solution with the negatively surface charged and electrostatically stabilized QD/silica particles leads to their attraction onto the pads by electrostatic interactions. An immersion time setting of 15mins is typical for a particle concentration on the order of 10¹²/cm³. For best result, solvents with moderate ionic strength are preferred to avoid overscreening of the electric field. A Debye screening length commensurate with composite particle size helps to improve binding specificity. Once a pad is occupied by a single silica-clad QD particle, Coulomb repulsion between the particles overpowers the attraction and in optimal conditions prevents a second particle attachment. Similarly, the silicon substrate carrying a net negative charge due to the hydrolysis of its native oxide surface also remains free of particles. Thus, by fine tuning the pad geometry for a given particle size, we have been able to achieve controlled placement of single QDs into individual sites with very high accuracy, as shown in the scanning electron microscope (SEM) images in Fig. 3(f).

To illustrate the influence of the pad sizes on the kinetics of the particle assembly and the quality of the final result, we varied the pad diameter D from 200nm to 400nm for QD/silica particles with diameter $d=220$ nm, as shown in Fig. 3(g)-3(j). We found that the particle capture probability decreased when D became smaller than d , whereas multiple particles could

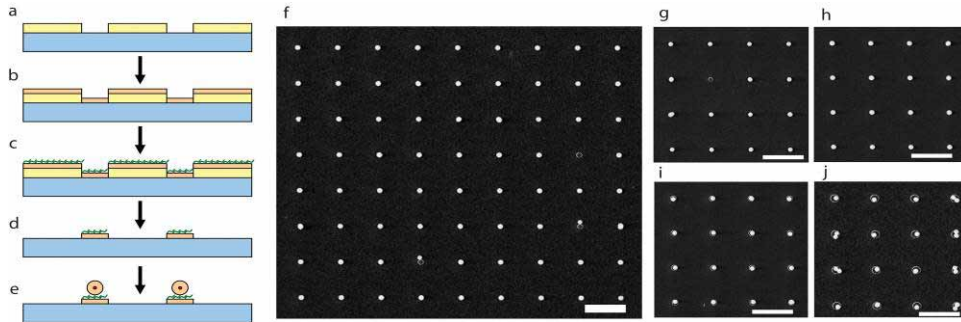


Fig. 3. (Media 3) Electrostatic force self-assembly of the silica-encapsulated QDs at single-particle resolution. a-e, schematics of the process flow of the electrostatic force self-assembly, which starts off with patterning of the PMMA resist on silicon substrate by electron-beam lithography (a), followed by deposition of SiO_2 film (20nm thick) by ion-beam sputtering (b) and assembly of a monolayer of polyelectrolyte (PDDA) molecules on the SiO_2 surface by dip-coating (c). Lift-off of the PMMA film in acetone leads to PDDA covered SiO_2 pad (d). Finally, immersion of the template into silica-clad QD ethanol solution results in spatially selective settlement of single silica-clad QD particle on each pad (e) via electrostatic interactions. f, scanning electron microscope image of a highly ordered array of individual silica-clad QDs formed by electrostatic force self-assembly. A small fraction of the particles are accidentally displaced from the target site, exposing the PDDA-covered SiO_2 pad underneath. g-j, SEM image examples of EFSA results when the pad size is varied from 200nm (g), 250nm (h), 300nm (i) to 400nm (j). The diameter of the silica-clad QD is 220nm. The scale bar in (f)-(j) is $2\mu\text{m}$.

be accommodated on a single pad when D was increased to nearly twice the size of the particles. For a wide window of parameter values in between, single particle capture probability up to 95% over macroscopic area ($>100\times 100\mu\text{m}^2$) was found, demonstrating a good tolerance of our method to the finite pad and particle size fluctuations from fabrication uncertainties.

It is worth noting that the EFSA method takes substantially less time (typically a few minutes) to implement in comparison to the assembly technique based on capillary forces [21] (typically a few hours, scaling with substrate size). It is also insensitive to fluctuations in parameters such as temperature and colloidal concentration. Furthermore, the fact that EFSA method relies on surface charge contrast rather than the trapping force exerted by the surface profile suggests certain flexibility in designing the template geometry for practical purposes. As a complementary method, we also developed well-shaped traps (as opposed to pads) within poly(methyl methacrylate) (PMMA) templates which could also capture single QD/silica particles as efficiently (not shown here).

2.3 Optical characterization of the assembled QDs

The optical properties of the geometrically arrayed single QDs were studied and characterized, firstly by fluorescence microscopy, and secondly, through photon statistical measurements, all at room temperature. Fig. 4(a) shows the confocal fluorescence microscope image collected from a square-lattice array of silica-clad QDs, which spans over an area of $80\times 80\mu\text{m}^2$ with $2\mu\text{m}$ pitch. It needs to be stressed that this particular planar geometry is chosen only for demonstration purpose. Virtually any pattern arrangement defined by

electron-beam lithography can be used to create the arrays. In acquiring the image, a 405nm laser diode excitation source and a single photon counting avalanche photodiode (APD) detector were used. Subsequent photon statistical analysis shows that the majority of the emitters sitting precisely at the lattice sites in the image correspond to single QDs (see next).

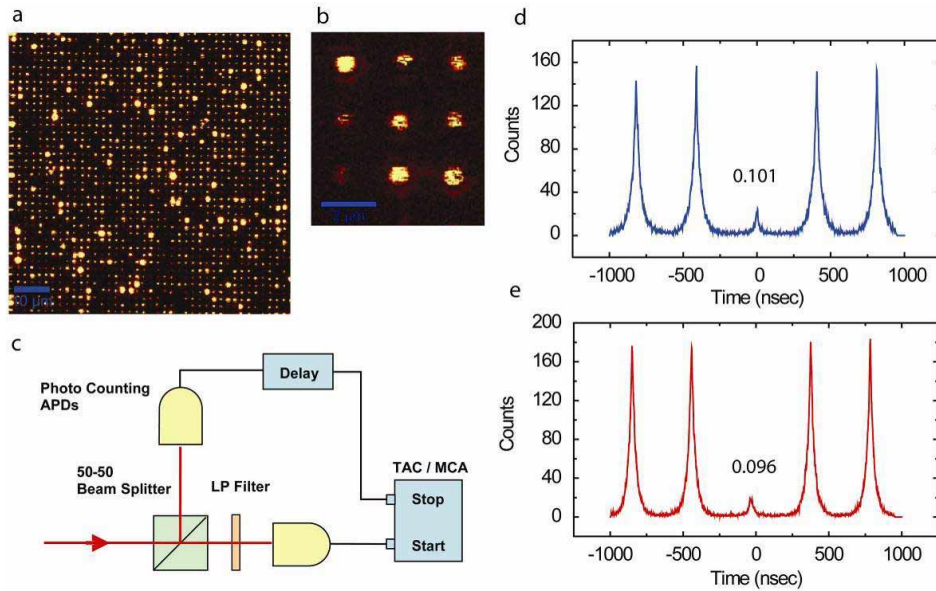


Fig. 4. (Media 4) Photon statistics measurement of the emission from single silica-encapsulated II-VI semiconductor colloidal QDs in self-assembled array. a, fluorescence image of an array of single silica-clad QDs captured by a confocal microscope. The particles reside on a square lattice with $2\mu\text{m}$ pitch. The scale bar is $10\mu\text{m}$. b, a close-up fluorescence image of a 3×3 silica-clad QD array. The confocal excitation/detection geometry allows easy optical access to any individual silica-clad QD in the array. The scale bar is $2\mu\text{m}$. c, the Hanbury-Brown and Twiss intensity correlation apparatus for photon statistics measurement of the QD emissions. The QDs are excited by a 2.5MHz pulsed diode source operating at 405nm. d,e, a typical photoluminescence intensity correlation histogram collected from a single silica-clad QD in the array at room temperature (d), in comparison to the similar data collected from a bare QD control (e). The number in the graph indicates the ratio of the area under the peak at zero time delay to the averaged area of the neighboring peaks.

Their fluorescence intensity variations are mostly inherited from the QD themselves, as similar level of fluctuations has been observed in our bare QDs that might links to the variation of QD sizes as well as the randomness of the QD crystal orientation [32]. There are also a small fraction of the spots (less than 7% of the total number) in the image which are significantly brighter than the others. These “defect” sites tend to be occupied by multiple QDs, either in a single composite particle or as a group of particles.

The ability to create ordered QD assemblies where inter-particle separation larger than the wavelength of light can be specified has given us an easy optical access to targeted individual quantum dots to evaluate their performance as *single photon emitters*. For this measurement, we illuminated the sample through our high resolution (N.A. =1.3) confocal microscope with a diode laser operating at 405 nm in pulsed mode (individual pulse width $\tau_p=70\text{ps}$) at 2.5MHz repetition rate. The collected photoluminescence was fed into a Hanbury-Brown and Twiss intensity correlation instrument as depicted in Fig. 4(c). In Fig. 4(d), a typical photoluminescence intensity correlation histogram acquired from a randomly chosen single silica-clad QD particle in the array is displayed. The suppression of the amplitude of the peak near zero time delay is a clear indication of the photon antibunching characteristics [7]. We

define the figure of merit here as the ratio of the area under this peak to the area of the neighboring peak, which yields $A(0)=0.101$. In other words, the probability of this silica-clad QD emitting a multiphoton state upon each triggered excitation is suppressed by an order of magnitude relative to a coherent laser source. The result is compared to the data collected from a bare control QD as shown in Fig. 4(e) with $A(0)=0.096$. The closeness of the two values demonstrates the compatibility of the silica encapsulation and the assembly processes with the goal of achieving single photon emission characteristics of the individual colloidal QDs. Incomplete suppression of $A(0)$ is attributed to the decreasing $(1/R^3)$ of Auger recombination rate as the QD radius R increases [14]. Smaller CdSe QDs ($R=1.8\text{nm}$) with emission peak at 570nm have shown significantly lower values $A(0)=0.04$ was reported by X. Brokmann et al [17].

3. Summary

In summary, we have successfully developed an experimental approach which holds the prospect of alleviating some of the major limitations currently associated with the patterning of sub-10nm sized nanoparticles at single particle resolution in precise geometries with long range order. This approach is made possible by employing novel methods to first encapsulate individual nanoparticles in large and uniformly sized silica particles via microemulsion growth, and subsequently self-assemble them into predefined patterns utilizing the electrostatic interactions in solution in a massively parallel fashion. While this method is potentially applicable to a wide variety of materials, a specific example based on II-VI colloidal QDs is given in this paper demonstrating how 2D single QD arrays can be created. These highly ordered QDs are readily accessible by confocal fluorescence microscopy for site-selective photoexcitation and collection of spontaneous emission. Most importantly, the effectiveness of these patterned QDs as single photon emitters has been demonstrated in practice at room temperature. We believe that the ability of precise spatial control of semiconductor colloidal QDs on a solid substrate will facilitate the study of these optically active nanoparticles, for example in promoting their integration with advanced microcavity structures and related optoelectronic devices as a possible avenue towards practical single-photon-on-command sources for quantum optical applications.

Acknowledgement

This research is supported by Department of Energy (Grant # ER 46387) and the National Science Foundation (Grant 0725740).